Microbiological Research 168 (2013) 91–98

Contents lists available at SciVerse ScienceDirect

Microbiological Research

journal homepage: www.elsevier.de/micres

Does doping with aluminum alter the effects of ZnO nanoparticles on the metabolism of soil pseudomonads?

Tommy Fang[a,1], Jean-Luc Watson[a,1], Jordan Goodman[a], Christian O. Dimkpa[a], Nicole Martineau[a], Siddhartha Das[c], Joan E. McLean[b], David W. Britt[d], Anne J. Anderson[a,*]

[a] Department of Biology, Utah State University, Logan, 84322-5305, United States
[b] Utah Water Research Laboratory, College of Engineering, Logan, Utah 84322-8200, United States
[c] Chemistry and Biochemistry Department, United States
[d] Biological Engineering Department, Utah State University, Logan, UT 84322-4105, United States

ARTICLE INFO

Article history:
Received 15 August 2012
Received in revised form 29 August 2012
Accepted 8 September 2012

Keywords:
Al-doped nanoparticles
Al ions
Phenazines
Pseudomonad
Siderophore
ZnO nanoparticles

ABSTRACT

Doping of ZnO nanoparticles (NPs) is being used to increase their commercialization in the optical and semiconductor fields. This paper addresses whether doping with Al alters how ZnO NPs at nonlethal levels modifies the metabolism of soil-borne pseudomonads which are beneficial in performing bioremediation or promoting plant growth. The differences in X-ray diffraction (XRD) patterns, observed between commercial ZnO and Al-doped ZnO NPs indicated the aluminum was present as Al NPs. Both particles aggregated in the bacterial growth medium and formed colloids of different surface charges. They had similar effects on bacterial metabolism: rapid, dose-dependent loss in light output indicative of temporary toxicity in a biosensor constructed in *Pseudomonas putida* KT2440; increased production of a fluorescent pyoverdine-type siderophore, and decreased levels of indole acetic acid and phenazines in *Pseudomonas chlororaphis* O6. Solubilization of Zn and Al from the NPs contributed to these responses to different extents. These findings indicate that Al-doping of the ZnO NPs did not reduce the ability of the NPs to alter bacterial metabolism in ways that could influence performance of the pseudomonads in their soil environment.

1. Introduction

Zinc oxide nanoparticles (ZnO NPs) are produced for many applications that vary from use as sunscreens and antimicrobials (Aydin and Hanley 2010; Gajjar et al. 2009; Wahab et al. 2010) to blue-opticoelectronic devices (Huang et al. 2001). Doping ZnO NPs, such as with aluminum (Al) (Suchea et al. 2007; Chen et al. 2008; Norris et al. 2008), is an approach to better tune their electrical and optical properties. The inclusion of Al in the NP structure alters crystalline quality as revealed by fluorescence and other spectral properties (Chen et al. 2008; Kumar et al. 2011). The studies in this paper compared traits of commercially produced Al-doped and nondoped-ZnO NPs. Characterization of the particles used scanning electron microscopy (SEM), X-ray diffraction (XRD) and atomic force microscopy (AFM). Absorption and fluorescence spectra were observed and particle charge was measured. Elemental composition and the release of soluble metals were assayed to aid in understanding whether Al-doping of ZnO NPs would affect bacterial metabolism.

We are interested in the effects of NPs on soil microbes to provide information on potential problems to the agricultural sector with contamination of soil by NP release. There is concern that contamination may have impacts on nontarget organisms. For instance, studies with ZnO, Al_2O_3 and TiO_2 NPs show toxicity toward the most abundant metazoa in soil, the nematode (Wang et al. 2009), as well as soil-borne and bacteria (Jiang et al. 2009). We find that ZnO NPs alter the metabolism of two root-colonizing pseudomonads, *Pseudomonas chlororaphis* O6 (*Pc*O6) and a modified isolate of *Pseudomonas putida* KT2440. Both of these pseudomonads, unlike some human pathogenic bacteria (Brayner et al. 2006; Jones et al. 2008) and an isolate of *Pseudomonas fluorescens* (Jiang et al. 2009), have high thresholds for killing by the ZnO NPs (Gajjar et al. 2009; Dimkpa et al. 2011a). At sublethal levels ZnO NPs cause metabolic changes in the pseudomonads. The KT2440 isolate was engineered to act as an energy biosensor emitting light from harboring a *luxAB* cassette (Gajjar et al. 2009). Exposure of the biosensor to ZnO NPs shows a temporary increase, and then a decline, in light output in a dose- and time-dependent manner (Gajjar et al. 2009). The temporary increase in light output is consistent with the expression of the *luxAB* genes being dependent

* Corresponding author. Tel.: +1 435 797 3407.
E-mail address: anne.anderson@usu.edu (A.J. Anderson).
[1] These two researchers contributed equally to the work.

0944-5013/$ – see front matter © 2012 Published by Elsevier GmbH.
http://dx.doi.org/10.1016/j.micres.2012.09.001

on a metal-activated promoter (Miller et al. 2009; Gajjar et al. 2009). With *Pc*O6, changes are seen in the production of secondary products: a decrease in indole-3-acetic acid (IAA) (Dimkpa et al. 2012a) and an increased production of a fluorescent pyoverdine-type siderophore (PVD) (Dimkpa et al. 2012b) occurs when cells of *Pc*O6 are grown in medium supplemented with ZnO NPs. Both IAA and siderophore production have significant roles in the function of *Pc*O6 as it colonizes root surfaces. IAA production improves plant growth up to a threshold level (Beyeler et al. 1999; Patten and Glick 2002). Siderophores inhibit growth of fungal pathogens and provide iron to plants under conditions of iron stress (Dimkpa et al. 2009; Kloepper et al. 1980; Vansuyt et al. 2007). Siderophores also are active as effectors of induced plant resistance (van Loon et al. 2008). Thus, improved plant performance is associated with production of both IAA and siderophore by *Pc*O6.

Investigations into the mechanisms by which the sublethal levels of NPs affect bacterial metabolism have included analysis of the role of the Zn ions that they release. Zn ions cause changes in light output in the biosensor *P. putida* strain, mimicking the effects of the NPs (Gajjar et al. 2009). At low doses, the Zn ions stimulate light output due to activation of the promoter driving genes conditioning light output. At higher concentrations, light output decreases in a time- and dose-dependent manner characteristic of a toxic response. However, as with exposure to the ZnO NPs, toxicity is temporary because the bacteria adapt so that the cells retain culturability (Gajjar et al. 2009). Although exposure to Zn ions increases siderophore production (Dimkpa et al. 2012b; Rossbach et al. 2002), the ions at the levels of solubilization did not explain reduced IAA production in *Pc*O6 when cultured with ZnO NPs (Dimkpa et al. 2012a).

The presence of additional materials in NPs can modify the antimicrobial effect of the NPs. For instance citrate and humic acid-coatings of Ag NPs limit their antimicrobial activity (Fabrega et al. 2009a,b). Changes in structure and spectral characteristics are documented between Al-doped and nondopedZnO NPs studied by Kumar et al. (2011). Lee et al. (2010) working with sand, with and without aluminum coatings demonstrate stronger binding to the coated sand by two bacteria. Thus we speculate that changes in binding due to Al-doping of ZnO NPs could alter their microbial effects. Although we do not know from the manufacturer the form of Al in the Al-doped NPs, several papers show that toxicity of Al_2O_3 (alumina) NPs differs between microbes (Jiang et al. 2009; Mukherjee et al. 2011; Bala et al. 2011). In contrast aluminum NPs appear to have lesser toxicity (Mukherjee et al. 2011). Doshi et al. (2008) indicate little effect on the metabolism of *Vibrio fischeri in vitro*, although inhibition is observed at a high concentration of the Al NPs in soil. Braydich-Stolle et al. (2010) report no effects of Al NPs on *Staphyloccusaureus* under study to better understand effects of inhaled NPs on immunity.

We anticipate that Al and Zn ions would be released from the NPs, and Al toxicity varies between bacteria (He et al. 2012a,b). In *P. fluorescens*, acquired tolerance is associated with changes in metabolism to reduce the effects of the Fe-deficiency induced by Al ions (Lemire et al. 2010). Al ions also inhibit IAA production but increase siderophore levels in different *Streptomyces* spp. (Dimkpa et al. 2008). Al ions promote the formation of PVD type siderophores in *Pseudomonas aeruginosa* (Greenwald et al. 2008; Braud et al. 2009). Thus it seems likely that the Al ions released from the doped NPs also would have effects on bacterial metabolism.

In this paper we extended the study of NP effects on bacterial metabolism to another beneficial trait of *Pc*O6, that of the production of phenazines (Spencer et al. 2003; Krishnan et al. 2007). Phenazines inhibit growth of some fungi, potentially restricting the pathogen-challenge of plants (Spencer et al. 2003; Krishnan et al. 2007; Mavrodi et al. 2012). *Pc*O6 produces three phenazines, phenazine-1-carboxylic acid, 2-hydroxyphenazine and 2 hydroxyphenazine-1-carboxylic acid when cultured under conditions of rich nutrition (Housley et al. 2009). The hydroxyphenazines account for the orange pigmentation of cultures of *Pc*O6 in rich medium (Housley et al. 2009). Thus, any impact of the NPs on phenazine formation could affect the behavior of *Pc*O6 in the soil. Additionally, to determine whether effects of Al-doping varied between bacteria, we compared the toxicity of the Al-doped NPs to that of ZnO NPs in the biosensor, *P. putida* KT2440 (Gajjar et al. 2009). In each of the bioassays, the effects of the ZnO and Al-doped NPs were assessed relative to those caused by addition of defined concentrations of Al and Zn ions based on measured levels of release of the metals from the NPs in the bacterial growth medium. Properties of the Al-doped ZnO NPs were compared to those of the ZnO NPs using different spectroscopic and microscopic techniques.

2. Materials and methods

2.1. Characterization of nanoparticles

The ZnO NPs and Al-doped ZnO NPs (6% Al) were obtained from Sigma Chemical Company (MO, USA) and were described as having a nominal size of <100 nm. SEM was performed using a FEI Quanta 200 Environmental SE microscope (SEM) with the control software package, xTM Microscope Control Quanta version 3.0.13, on the dry materials; at least five images at different magnifications were recorded. Elemental analysis was performed with the same instrumentation using the software Energy Dispersive X-ray (EDAX) Spectroscopy Genesis Spectrum, version 5.959. Atomic force microscopy (AFM) analysis using a Nanoscope III Bioscope (Digital Instruments, Inc.) as described in Dimkpa et al. (2011b) was performed with dried samples from freshly prepared suspensions in double distilled deionized (dd) water or modified Lysogeny Broth (LB) prepared without NaCl with 10 g tryptone and 5 g yeast extract/L. Powder X-ray diffractions (XRDs) of the commercial nanopowders were recorded with RigakuMiniflex II with a Cu X-ray tube; the machine was fitted with a diffracted beam monochromator for Cu-radiation. Each spectrum was recorded at a scan speed of 4.0000°/min with a step width of 0.02°. Spectral peaks were compared with the database provided by the International Center for Diffraction Data (ICDD).

The surface charge of particles was determined using suspensions of 12.5 mg Zn/L of Al–ZnO NPs and ZnO NPs in dd water (pH = 7.72) or modified LB (pH 7.4) in a Zeta Meter (Zeta Meter, Inc., Staunton, VA, USA). Suspensions of the NPs in water, modified LB and ethanol were examined for absorbance and fluorescence using a Synergy4 Hybrid Multi-Mode Microplate Reader (BioTek, Inc., Winooski, VT, USA) with 325 nm excitation (Kumar et al. 2011). Metal release from the NPs in water and medium was determined by inductively coupled plasma mass spectrometry (ICP-MS) (Agilent 7500c) in the aqueous phase generated by two successive centrifugations of the NP suspensions at $15{,}500 \times g$ for 30 min. Based on the size and density of the NPs and the viscosity of the liquid, the minimum time required to precipitate the NPs would be 5 min under these conditions (Dimkpa et al. 2012a). Elemental composition of the NPs was determined by dissolving the NPs in 50% nitric acid and analysis by ICP-MS.

2.2. Bacterial growth conditions

Cells of *P. chlororaphis* O6 (*Pc*O6) and *P. putida* KT2440 biosensor were stored in 15% glycerol at −80 °C before use. *Pc*O6 cultures were generated from these stocks using an inoculum of 10^4 cells/ml in modified LB. Cultures were shaken at 150 rpm at 26 °C under room light for three days. The biosensor cells were raised in a minimal medium (MM) and suspended in dd sterile water for studies of light

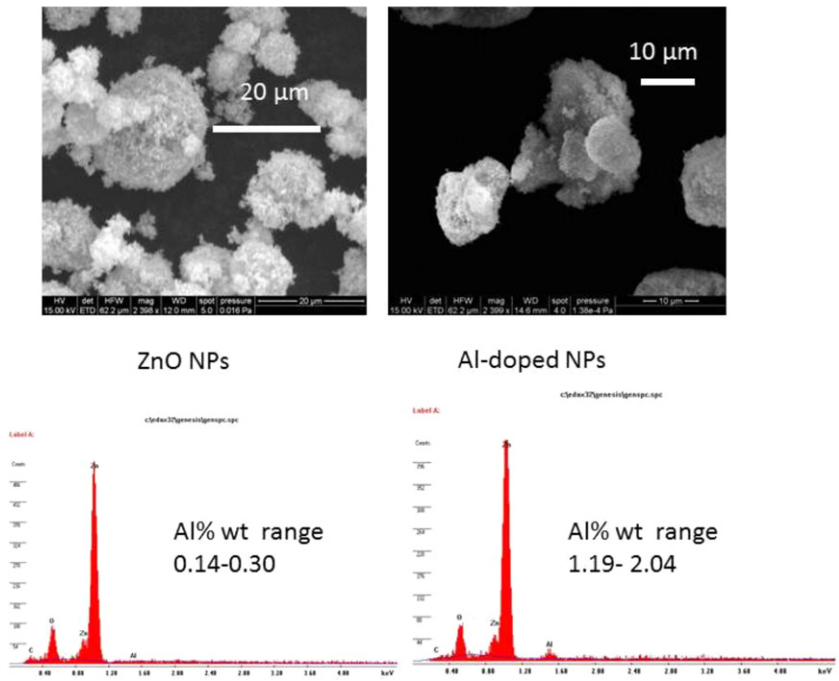

Fig. 1. SEM images and EDAX analysis of the ZnO NPs and Al-doped NPs. The SEM images were typical of the twenty fields of view examined. The EDAX analyses were based on five fields of view (only the Zn L peaks are shown in these images to aid in seeing the Al peak).

output as described in Gajjar et al. (2009). Cultures were amended with ions and NPs as designated.

Cell densities of cultures were determined by plating serial dilutions onto modified LB solidified with 2% agar. Colonies were counted 2 days after growth at 26 °C.

2.3. Determination of fluorescent siderophore, IAA and phenazine production by PcO6

Production of the fluorescent pyoverdine (PVD)-like siderophore was determined by measurement of characteristic fluorescence generated between 460 and 490 nm with excitation at 398 nm (Del Olmo et al. 2003) in a Synergy4 Hybrid Multi-Mode Micro plate Reader (BioTek, Inc., VT, USA). The culture medium was centrifuged at 15,000 × *g* for 10 min to remove cells and NPs and treated with an equal volume of ethyl acetate. The extracted medium was sampled for fluorescence determined by regulating the sensitivity levels of the instrumentation as required. IAA production was assessed by chromogen formation with Salkowski's reagent (Patten and Glick 2002) with the cell free cultures generated in the LB medium that was amended with 100 µg/ml tryptophan as the precursor (Dimkpa et al. 2012a). Phenazine levels were assessed after extraction of the cell-free culture medium into acidified ethyl acetate as described by Housley et al. (2009).

2.4. Determination of the effect of NPs and ions on light output from the biosensor in P. putida KT2440

The *P. putida* biosensor strain (Gajjar et al. 2009) was stored in 15% glycerol at −80 °C and grown to stationary phase in liquid MM containing per L: K_2HPO_4 10.5 g, KH_2PO_4 4.5 g, sodium citrate ($2H_2O$) 0.5 g, $(NH_4)_2SO_4$ 1.0 g, sucrose 20 g and $MgSO_4$ 0.1 g (Gajjar et al. 2009). After regrowth of overnight cultures in MM, cells suspended in sterile deionized distilled water (200 µl at 1×10^8 cells/ml) were loaded into 96-well plates and examined in the presence and absence of defined concentrations of ions or NPs. Light output generated by the presence of *luxAB* genes within the biosensor (Gajjar et al. 2009) was measured at 10 min intervals for one h in a LMaxII384 Molecular Device luminometer (Molecular Devices Corporation, Sunnyvale CA) with Softmax Pro V. 4.7 software. Each treatment condition was performed with at least three different experiments each with triplicate readings of one sample. Culturability of the cells after the 1 h of exposure to NPs or ions was determined by dilution plating onto LB agar medium and counting colonies after 2 days incubation at 26 °C.

3. Results

3.1. Characterizations of NPs

The scanning electron micrographs of the ZnO NPs imaged from the dried powder showed clustering of NPs into larger aggregates (Fig. 1). The agglomerated particles of the Al-doped NPs appeared slightly smoother than those of the ZnO NPs (Fig. 1). Elemental analysis by EDAX of the material confirmed that the Al-doped particles had higher concentrations of Al (1.9–2.3% by weight) than the non-doped particles (Fig. 1). No peaks other than for the elements Zn, O and Al were observed indicating the purity level of the products. Elemental analysis of the particles using ICP-MS confirmed over a 2300-fold greater level of Al in the Al-doped ZnO NPs than the non-doped particles (Table 1). The values for other contaminants of the NPs (Table 1) showed differences between the two preparations

Table 1
Elemental analysis of Al-doped and ZnO NPs.

Element	Al-doped ZnO NPs (µg/g)	ZnO NPs (µg/g)
Al	3639 ± 14	1.58 ± 0.45
Fe	0.01 ± 0.00	4.46 ± 1.43
Cu	<1	<1
Zn	789,000 ± 25,000	788,000 ± 55,000
Cd	1.49 ± 0.9	1.44 ± 0.01
Pb	12.5 ± 0.4	5.3 ± 0.04

Data are based on replicate samples.

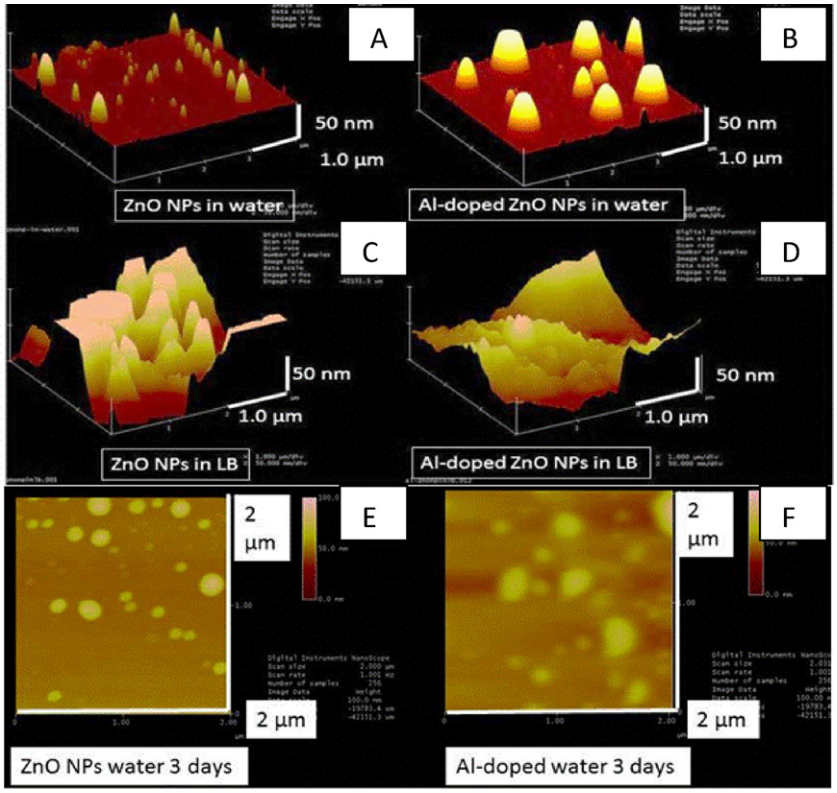

Fig. 2. AFM images of NPs after 3 days suspension in water or LB medium. The images are typical of 5 images at the same magnifications. (A), (C) and (E) are images for the ZnO NPs and (B), (D) and (F) for the Al-doped NPs.

although these elements were at low levels. Individual nano-sized particles were observed with both NPs by AFM imaging from water suspensions, but these were obscured into large micro structures after suspension in LB (Fig. 2). Top views showed that the particles dried from water suspensions were round.

XRD analyses revealed differences in the crystallites of the Al-doped and undopedZnO NPs (Fig. 3). The diffraction pattern for the ZnO NPs was that expected from the wurzite structure found in zincite (DB card number 00-005-066). The wurzite structure is not favored in bulk minerals, but is formed with some NPs, including ZnO. This spectrum revealed small peaks characteristic of Al NPs and was consistent with the ICP-MS elemental analysis showing traces of Al in the commercial ZnO NPs. However, the diffraction pattern from the Al-doped ZnO NPs was distinct (Fig. 3) with strong diffractions at $2\theta = 37.9^\circ$, 44.1° and 77.4° that are characteristics of Al NPs (DB card number 00-004-0787). The lack of diffraction below $2\theta < 30$ indicated that the size of Al NP would be >20 nm (Ref: *US Research Nanomaterials*, stock# US1052). Thus, in the Al-doped ZnO NPs, Al was present as chemically distinct Al-crystallites.

The absorption and fluorescent spectra of the particles in water are shown in Fig. 4. In both water and LB (data not shown) the absorbance spectra showed a defined peak for the ZnO NPs at 375 nm compared with a rounded shoulder between 360 and 370 nm for the Al-doped NPs (Fig. 4A). However, in water there was a defined emission band at 375 nm with smaller fluorescence maxima into the visible wavelengths (*e.g.* 435 nm) for the ZnO NPs. The fluorescence emission spectrum was much weaker for the Al-doped NPs (Fig. 4B).

The Al-doped NPs displayed different surface charges to the ZnO NPs. In water the Al-doped NPs had a positive charge (39.2 ± 2.1 mV) whereas the LB medium neutralized charge. By eye, the Al-doped NPs precipitated in the LB medium faster than in water. The ZnO NPs had similar negative charges in both water (-24.0 ± 1.6 mV) and LB medium (-20.3 ± 1.8 mV) at pH 7.15.

Both Zn and Al were solubilized from the NPs during cellular growth as shown in Table 2. The levels of soluble Zn were similar in the LB cultures whether the ZnO or the Al-doped ZnO NPs were used. The levels of soluble metal were greater in LB than when the particles were suspended in water (Table 2).

Table 2
Soluble aluminum and zinc in water or LB medium after three days with shaking with or without inoculation with *Pc*O6 and the addition of ZnO or Al-doped ZnO NPs at 500 mg Zn/L.

Sample	LB				Water	
	Without cells		With cells		Without cells	
	Al (mg/L)	Zn (mg/L)	Al (mg/L)	Zn (mg/L)	Al (mg/L)	Zn (mg/L)
No additions	0.04 ± 0.003	1.0 ± 0.1	0.03 ± 0.01	1.0 ± 0.1	<0.004	<0.001
ZnO NPs 500 mg/L	0.02 ± 0.005	95 ± 7	0.04 ± 0.003	100 ± 20	0.01 ± 0.003	6.01 ± 0.01
Al-doped NPs 500 mg/L	0.126 ± 0.003	126 ± 15	0.07 ± 0.02	111 ± 17	0.01 ± 0.003	6.03 ± 0.01

Soluble Zn and Al were determined using ICP-MS analysis of two replicates for each sample.

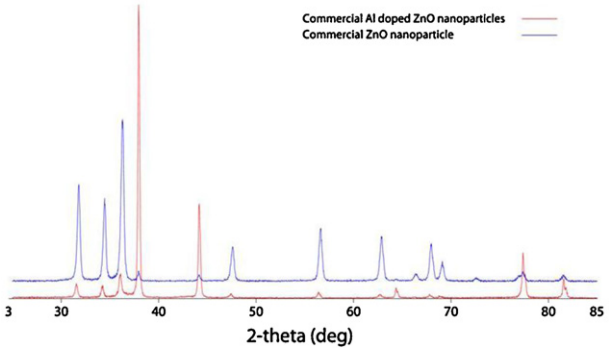

Fig. 3. Powder XRD spectra of Al-doped and nondoped ZnO NPs.

Table 3
Effect of addition of ZnO, Al-doped ZnO NPs and ions on *Pc*O6 culturability on LB medium.

Cell culture	CFU/mL × 10^9
Control	7.0 ± 3.0
ZnO NPs	4.6 ± 1.0
Al-doped ZnO NPs	4.0 ± 2.0
Zn ions 120 mg/L	4.0 ± 1.5
Al ions 0.5 mg/L	5.0 ± 1.0

CFU, culture forming units. Cultures were grown for three days before plating to determine culturability and pigmentation on LB plates. Data are typical of three independent studies.

3.2. Effects of ZnO and Al-doped ZnO NPs on growth and metabolism of PcO6

Amendment of the LB cultures with ZnO and Al-doped ZnO NPs did not change the extent of cell culturability after 3 days of incubation; all flasks in stationary phase averaged over 10^9 cells/ml (Table 3). The pH of the cultures at harvest (pH 8.1 ± 0.1) was not affected by the treatments with NPs or ions. Production of fluorescence typical of the pyoverdine-type siderophores (emission 460–480 nm with 398 nm excitation) was enhanced by the Al-doped ZnO NPs as well as ZnO NPs (Fig. 5A). Promotion of siderophore levels by Al-doped NPs and Al ions was confirmed in an iron-deficient siderophore-inducing-medium (SIM) (Dimkpa et al. 2012b). SIM was used previously to demonstrate induction by ZnO NPs (Dimkpa et al. 2012b) (data not shown). Amendment of LB with 120 mg/L Zn ions, to represent levels of soluble Zn released from the NPs, resulted in fluorescence levels similar to the unamended cultures. Production of IAA, as detected by positive chromogen production by Salkowski's reagent, by *Pc*O6 was very low in the LB medium (Fig. 5B). However, the levels were reduced further in LB medium containing either ZnO NPs or the Al-doped NPs. Use of SIM (Dimkpa et al. 2012a) confirmed that the Al-doped NPs reduced IAA formation (data not shown). In LB medium, ion release from the NPs could contribute to the reduced IAA levels; repression in chromogen production was observed with 120 mg/L Zn ion treatment and Al ions at 0.5 mg/L.

The LB medium was used as the growth medium because it supported strong production of phenazines by *Pc*O6 (Fig. 5C and D). Amendment with the ZnO or Al-doped ZnO NPs reduced the characteristic orange pigmentation in the *Pc*O6-LB cultures to similar extents (Fig. 5D). Addition of Zn ions at 120 mg/L strongly reduced orange pigmentation whereas this was retained to a higher degree with amendments of 0.5 mg/L Al ions (Fig. 5C). Extraction of the culture medium and cells into acidified ethyl acetate showed that much of the orange pigmentation, due to 2-hydroxyphenazine, was retained at the water:ethyl acetate interface. Thus, the extracted preparations were yellow-colored. The absorbance readings of the extracts showed that the Al-doped ZnO NPs and the ZnO NPs inhibited phenazine accumulation in the cell pellet as well as their secretion. Strong inhibition of phenazine production occurred with the presence of Zn ions. The Al ions had less of an inhibitory effect.

3.3. Effects of Al-doped NPs and Al ions on biosensor activity in a modified strain P. putida KT2440

Light output of the biosensor cells derived in pseudomonad strain *P. putida* KT2440 changed to similar extents in treatments with the Al ZnO NPs as with the ZnO NPs (Fig. 6). The toxicity was time- and dose-dependent as illustrated by responses to the 20 and 200 mg Zn exposure from NPs (Fig. 6A). With both NPs, there was immediate increase in light output followed by decline. Culturability of the cells did not differ between treatments ($2.3 \pm 1.5 \times 10^8$ cells/ml).

The early increase in light output seen with the NPs was duplicated by exposure of the biosensor to Zn ions at 0.5 and 1 mg/L (Fig. 6B). Al ions, 0.1 and 0.5 mg/L, also increased light output but with a slower time profile than for the instant response to Zn ions. None of the ion treatments altered cell culturability (data not shown).

4. Discussion

Elemental analysis by ICP-MS of acid digests and by EDAX confirmed the presence of Al in the Al-doped particles, although the level we detected was lower than the 6% value provided by the manufacturer. The Al-doping did not dramatically alter the appearance of the particles as revealed by SEM and AFM microscopy. However, XRD analysis of the powders showed that the Al-doped particles contained large (>20 nm) Al NPs indicating that the normal crystallinity of the ZnO NPs to a wurzite-structure was disrupted. This type of impurity was present in the commercial ZnO NPs to a small extent as revealed by overlapping spectral peaks and this finding agreed with the detection of trace levels of Al in the product by ICP-MS analysis of its acid digest (see also Dimkpa et al. 2012c). Thus, this commercial product has a mix of ZnO NPs and as defects,

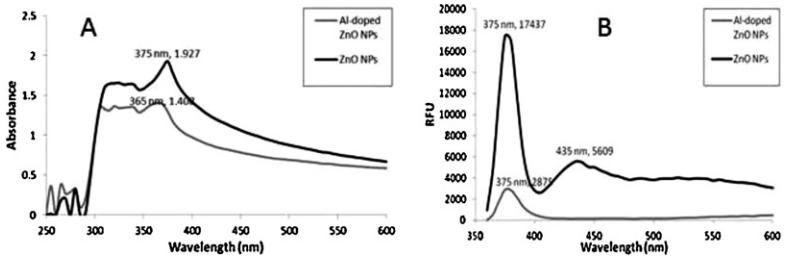

Fig. 4. Absorbance (A) and fluorescence spectra (B) in water of NPs. The fluorescence spectra were generated with excitation wavelength of 325 nm according to Kumar et al. (2011).

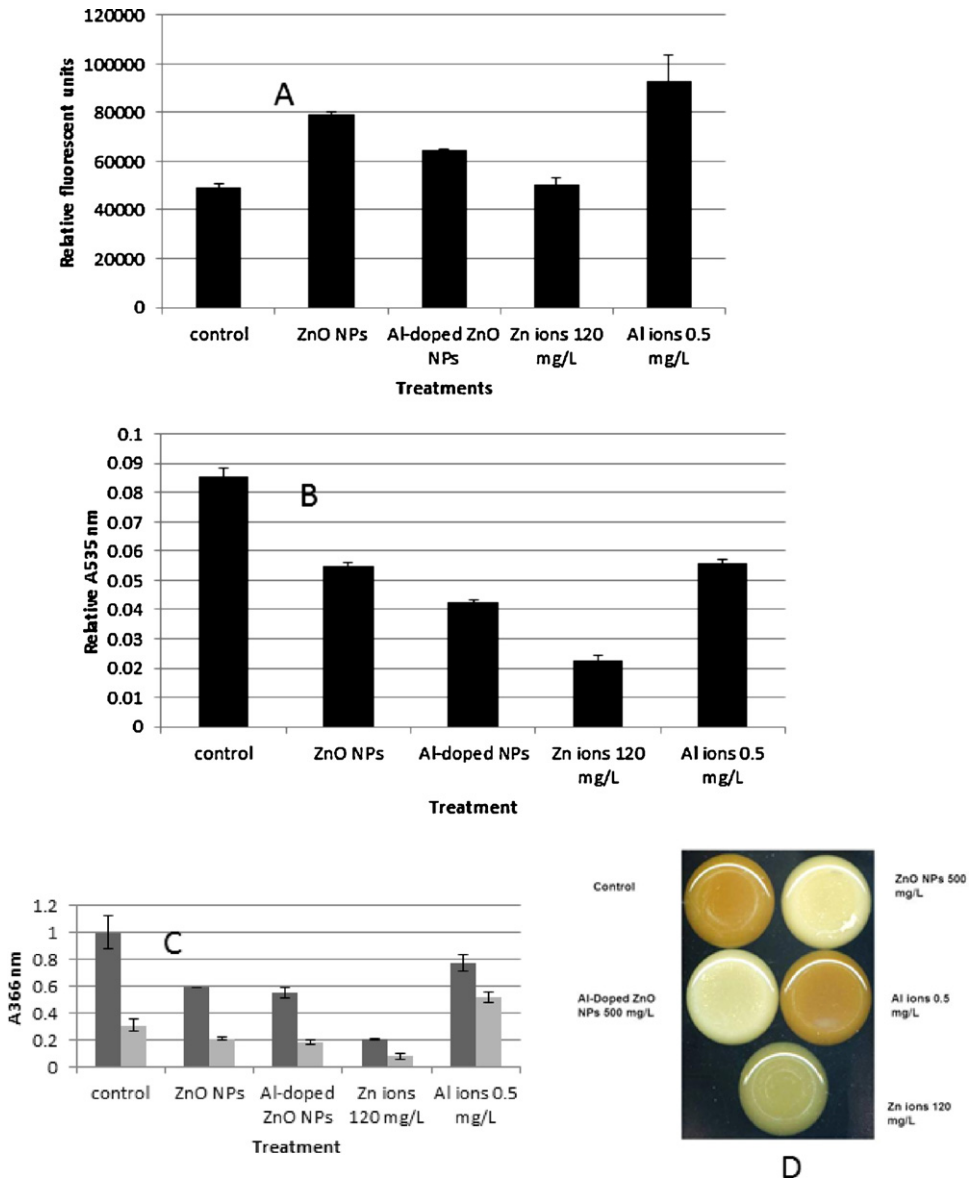

Fig. 5. Effects of amendments with NPs and ions on production by *Pc*O6 of (A) fluorescent siderophore, (B) IAA, (C) phenazine and (D) an image to show differential pigmentation in the cultures at harvest. Data are from 3 day-old cultures in LB medium and are means from two separate cultures with standard deviation. The data are typical of at least three different independent studies. The siderophore data were based on measuring fluorescence (relative units) of 1000-fold diluted samples with excitation at 398 nm and emission at 470 nm (Dimkpa et al. 2012b). IAA was measured as described in Patten and Glick (2002) by reading chromogen formation at 535 nm. In Fig. 3C absorbance due to phenazines was read at 366 nm for 1–10 diluted samples of the secreted products (dark bars) and undiluted extracts from the cells (lighter bars).

aluminum Al NPs, whereas the products studied by Kumar et al. (2011) had regions where Al replaced Zn in the crystallites of ZnO.

Changes in surface charge of the colloids developed by the NPs in suspension were apparent. Doping with Al caused slight shifts in the absorbance spectrum, as was previously observed by Kumar et al. (2011) with Al-doped particles. The Al-doped particles also showed a different fluorescence spectrum with less emission in the visible wavelengths than that for the ZnO NPs. The presence of an emission peak at 375 nm confirmed the data published by Chen et al. (2008) for ZnO NPs. However, with their Al-doped ZnO NPs there was a shift to an absorbance maxima at 380–386 nm (Chen et al. 2008), although these changes were not apparent for the Al-doped particles prepared by Kumar et al. (2011). Possibly different methods of synthesis affected how the dopant was integrated into the ZnO particles, resulting in the changes in properties from these two groups (Chen et al. 2008; Kumar et al. 2011) as well as from the commercial preparations used in our studies.

Solubilization studies indicated that the Al-doped particles would act as a point source for both Al and Zn ions, although the release concentrations of Al ions were very low, consistent with the small extent of doping from the Al-doped NPs. The amounts of soluble Zn released from both particles during cell growth were similar. In LB medium the measured solubilization of Zn metal was over ten-fold higher than in water, perhaps because organic material, such as —SH and histidine-containing proteins, would hold the ions in a soluble form.

In each of the assays designed to test effects on metabolism in soil pseudomonads, the Al-doped and ZnO NPs behaved similarly when used at equivalent doses of Zn. In *Pc*O6, we found similar inhibition of IAA production and enhanced siderophore levels in cultures amended with the Al-doped ZnO NPs as the undoped NPs (Dimkpa et al. 2012a,b). We also documented similar major changes in phenazine production caused by the Al-doped particles and the ZnO NPs. The engineered biosensor in *P. putida* KT2440 showed

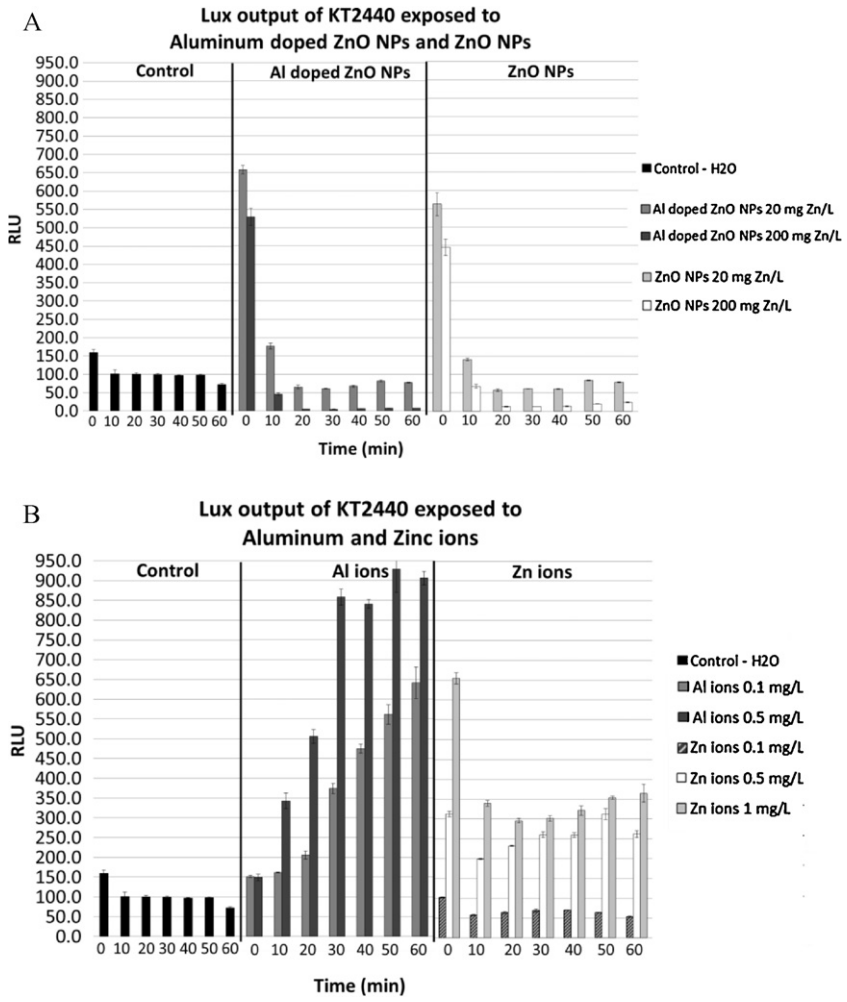

Fig. 6. Effects of NPs and ions on light output from biosensor constructed in *P. putida* KT2440. (A) Comparison of effects of ZnO NPs and Al-doped NPs and (B) Effects of Al and Zn ions at the designated doses. Data are the means of three replicates with standard errors and are typical of three independent studies. Light output is shown as relative light units (RLU).

dose-dependent responses with transient increased light output followed by decreases in the 60 min exposure period for both NPs.

The similar levels of soluble Zn from both NPs in part can explain the identical nature of the bacterial responses to the doped and undoped particles. However, our work also showed the added potential role of released Al from the Al-doped NPs. The Al ions increased secretion of the PVD siderophore and decreased IAA levels produced by *Pc*O6. This finding corroborates studies with *Streptomyces* spp. in which Al ions differential affected IAA and siderophore production (Dimkpa et al. 2008). We posit that the change in siderophore levels was consistent with induction of Fe stress in the bacterial cells when exposed to Al ions, as has been reported for *P. fluorescens* (Lemire et al. 2010).

Only the release of Zn, however, appeared to be involved in the reduction of phenazines in *Pc*O6 by the Al-doped and the ZnO NPs. Al ions used at a level near to the released level were not inhibitory to phenazine production. While this work was in progress Li et al. (2011) reported that the activity of the first committed enzyme in phenazine biosynthesis in *Burkholderialata* 383, PhzE, was inhibited by Zn ions when assayed with the highly purified protein. Thus, we speculate that inhibition of the activity of the enzyme PhzE could be one mechanism by which Zn inhibited phenazine production in *Pc*O6. Working with the highly purified enzyme is beyond the scope of the present study, and we speculate that it may not be possible to see effects with crude extracts because of speciation of Zn with materials present in the extracts. Additionally our visual analysis suggested that production of the orange hydroxyphenazines rather than the yellow phenazine carboxylate also was affected by the Zn rather than the Al ions. The hydroxyphenazine is produced from the phenazine-1-carboxylic acid by a specific monooxygenase (Delaney et al. 2001).

Our findings add to the growing body of knowledge that contamination of soils with NPs could influence the functioning of the biota. For instance, Wang et al. (2009) and Jiang et al. (2009) have shown that soil Gram-negative and Gram-positive bacteria and the eukaryotic nematodes are sensitive to the toxicities of ZnO, Al_2O_3 and TiO_2 NPs. Other papers also discuss the antimicrobial activity of Al_2O_3 (However, inhibition of growth of plant pathogenic fungi by NPs (He et al. 2012a,b; Jayaseelan et al. 2012) has led to the speculation that NPs may be formulated in pesticides for plant disease control. Currently, it is difficult to predict the given risk of NP-contamination in a soil because there are many different aspects that are poorly understood about the fate of NPs in soil. Our data suggest that both the NPs and ions released from the NPs could have important consequences in ecosystem function.

In summary, although differences in physical properties were observed between commercial Al-doped ZnO NPs and ZnO NPs, both materials behaved similarly in influencing metabolic changes in two soil-borne pseudomonads. These findings may relate to cells reacting to the similar levels of Zn released from both NPs. Our findings suggested that contact between soil microbes and both metal oxide NPs would lead to changes in metabolism of

significance to the survival and the behavior of the bacterium. Temporary loss in energy status and altered levels of environmentally significant products, IAA, a fluorescent siderophore, and phenazines, were demonstrated when the microbes were challenged with the NPs.

Acknowledgements

Support from the USDA (CSREES grant 2011-03581), the Utah Agricultural Experiment Station (AES) and the Utah Water Research Laboratory is gratefully acknowledged. AES Journal Paper Number 8441.

References

Aydin SB, Hanley L. Antibacterial activity of dental composites containing zinc oxide nanoparticles. J Biomed Mater Res B Appl Biomater 2010;94:22–31.

Bala T, Armstrong G, Laffir F, Thornton R. Titania-silver and alumina-silver composite nanoparticles: novel, versatile synthesis, reaction mechanism and potential antimicrobial application. J Colloid Interface Sci 2011;356:395–403.

Beyeler M, Keel C, Michaux P, Haas D. Enhanced production of indole-3-acetic acid by a genetically modified strain of *Pseudomonas fluorescens* CHA0 affects root growth of cucumber, but does not improve protection of the plant against *Pythium* root rot. FEMS Microbiol Ecol 1999;28:225–33.

Braydich-Stolle LK, Speshock JL, Castle A, Murdock RC, Hussain SM. Nanosized aluminum altered immune function. ACS Nano 2010;4:3661–70.

Braud A, Hoegy F, Jezequel K, Lebeau T, Schalk IJ. New insights into the metal specificity of the *Pseudomonas aeruginosa* pyoverdine-iron uptake pathway. Environ Microbiol 2009;11:1079–91.

Brayner R, Ferrari-Iliou R, Brivois N, Djediat S, Benedetti MF, Fievet F. Toxicological impact studies based on *Escherichia coli* bacteria in ultrafine ZnO nanoparticles colloidal medium. Nano Lett 2006;6:66–870.

Chen KJ, Fang TH, Hung FY, Ji LW, Chang SJ, Young SJ, Hsiao YJ. The crystallization and physical properties of Al-doped ZnO nanoparticles. Appl Surf Sci 2008;254:5791–5.

Delaney SM, Mavrodi DV, Bonsall RF, Thomashow LS. phzO, a gene for biosynthesis of 2-hydroxylated phenazine compounds in *Pseudomonas aureofaciens* 30-84. J Bacteriol 2001;183:318–27.

Del Olmo A, Caramelo C, SanJose C. Fluorescent complex of pyoverdin with aluminum. J Inorg Biochem 2003;97:384–7.

Dimkpa CO, Svatoš A, Dabrowska P, Schmidt A, Boland W, Erika K. Involvement of siderophores in the reduction of metal-induced inhibition of auxin synthesis in *Streptomyces* spp. Chemosphere 2008;74:19–25.

Dimkpa CO, Merten D, Svatoš A, Büchel G, Kothe E. Siderophores mediate reduced and increased uptake of cadmium by *Streptomyces tendae* F4 and sunflower (*Helianthus annuus*), respectively. J Appl Microbiol 2009;107:1687–96.

Dimkpa CO, Calder A, McLean JE, Britt DW, Anderson AJ. Responses of a soil bacterium *Pseudomonas chlororaphis* O6 to commercial metal oxide nanoparticles compared with responses to metal ions. Environ Pollut 2011a;159:1749–56.

Dimkpa CO, Calder C, Gajjar P, Merugu S, Huang W, Britt DW, McLean JE, Johnson WP, Anderson AJ. Interaction of silver nanoparticles with an environmentally beneficial bacterium *Pseudomonas chlororaphis*. J Hazard Mater 2011b;188:235–428.

Dimkpa CO, Zeng J, McLean JE, Britt DW, Zhan J, Anderson AJ. Production of indole-3-acetic acid via the indole-3-acetamide pathway in the plant-beneficial bacterium *Pseudomonas chlororaphis* O6 is inhibited by ZnO nanoparticles but enhanced by CuO nanoparticles. Appl Environ Microbiol 2012a;78:1404–10.

Dimkpa CO, McLean JE, Britt DW, Anderson AJ. CuO and ZnO nanoparticles differently affect the secretion of fluorescent siderophores in the beneficial root colonizer *Pseudomonas chlororaphis* O6. Nanotoxicology 2012b;6:635–42.

Dimkpa CO, McLean JE, Latta DE, Manangón E, Britt DW, Johnson WP, Boyanov MI, Anderson AJ. CuO and ZnO nanoparticles: phytotoxicity, metal speciation and induction of oxidative stress in sand-grown wheat. J Nanopart Res 2012c., http://dx.doi.org/10.1007/s11051-012-1125-29.

Doshi R, Braida W, Christodoulatos C, Wazne M, O'Connor G. Nano-aluminum: transport through sand columns and environmental effects on plants and soil communities. Environ Res 2008;106:296–303.

Fabrega J, Fawcett SR, Renshaw JC, Lead JR. Silver nanoparticle impact on bacterial growth: effect of pH, concentration, and organic matter. Environ Sci Technol 2009a;43:7285–90.

Fabrega J, Renshaw JC, Lead JR. Interactions of silver nanoparticles with *Pseudomonas putida* biofilms. Environ Sci Technol 2009b;43:9004–9.

Gajjar P, Pettee B, Britt DW, HuangW, JohnsonWP, Anderson AJ. Antimicrobial activities of commercial nanoparticles against an environmental soil microbe, *Pseudomonas putida* KT2440. J Biol Eng 2009;3:9, http://dx.doi.org/10.1186/1754-1611-3-9.

Greenwald J, Zeder-Lutz G, Hagege A, Celia H, Pattus F. The metal dependence of pyoverdine interactions with its outer membrane receptor FpvA. J Bacteriol 2008;190:6548–58.

He G, Lin J, Liu Q, Zhang J, Wu J. The effects of aluminum stress on bacterial community diversity in acidic red soils by polymerase chain reaction (PCR)-amplified restriction fragment length polymorphism Afr. J Microbiol Res 2012a;6:3707–15.

He L, Liu Y, Mustapha Z, Lin M. Antifungal activity of zinc oxide nanoparticles against *Botrytis cinerea* and *Penicillium expansum*. Microbiol Res 2012b;166:207–15.

Housley L, Anderson T, Sontag N, Han S-H, Britt DW, Anderson AJ. Pluronics' influence on pseudomonad biofilm and phenazine production. FEMS Microbiol Lett 2009;293:148–53.

Huang M, Mao S, Feick H, Yan H, Wu Y, Kind H, Weber E, Russo R, Yang P. Room-temperature ultraviolet nanowire nanolasers. Science 2001;292:1897–9.

Jayaseelan C, Rahuman AA, Kirthi AV, Marimuthu S, Santhoshkumar T, Bagavan A, Gaurav K, Karthik L, Rao KV. Novel microbial route to synthesize ZnO nanoparticles using *Aeromonas hydrophila* and their activity against pathogenic bacteria and fungi. Spectrochim ACTA Part A-Mol Biomol Spectr 2012;90:78–84.

Jiang W, Mashayekhi H, Xing B. Bacterial toxicity comparison between nano- and micro-scaled oxide particles. Environ Pollut 2009;157:1619–25.

Jones N, Ray B, Ranjit KT, Manna AC. Antibacterial activity of ZnO nanoparticle suspensions on a broad spectrum of microorganisms. FEMS Microbiol Lett 2008;279:71–6.

Kloepper JW, Leong J, Teintze M, Schroth MN. Enhanced plant growth by siderophores produced by plant growth-promoting rhizobacteria. Nature 1980;286:885–6.

Krishnan HB, Kang BR, Krishnan HA, Kim KY, Kim YC. *Rhizobium etli* USDA9032 engineered to produce a phenazine antibiotic inhibits the growth of fungal pathogens but is impaired in symbiotic performance. Appl Environ Microbiol 2007;73:327–30.

Kumar RS, Sathyamoorthy R, Sudhagar P, Matheswaran P, Hrudhya CP, Kang YS. Effect of aluminum doping on the structural and luminescent properties of ZnO nanoparticles synthesized by wet chemical method. Physica E Low-dimens Syst Nanostruct 2011;43:1166–70.

Lee CG, Park SJ, Han YU, Park JA, Kim SB. Bacterial attachment and detachment in aluminum-coated quartz sand in response to ionic strength change. Water Environ Res 2010;82:499–505.

Lemire J, Mailloux R, Auger C, Whalen D, Appanna VD. Pseudomonas fluorescens orchestrates a fine metabolic-balancing act to counter aluminium toxicity. Environ Microbiol 2010;12:1384–90.

Li QA, Mavrodi DV, Thomashow LS, Roessle M, Blankenfeldt W. Ligand binding induces an ammonia channel in 2-amino-2-desoxyisochorismate (ADIC) synthase PhzE. J Biol Chem 2011;286:18213–21.

Mavrodi DV, Mavrodi OV, Parejko JA, Bonsall RF, Kwak YS, Paulitz TC, Thomashow LS, Weller DM. Accumulation of the antibiotic phenazine-1-carboxylic acid in the rhizosphere of dryland cereals. Appl Environ Microbiol 2012;78:804–12.

Miller CD, Pettee B, Zhang C, Pabst M, McLean JE, Anderson AJ. Copper and cadmium: responses in *Pseudomonas putida* KT2440. Lett Appl Microbiol 2009;49:775–83.

Mukherjee A, Sadiq LM, Prathna TC, Chandreasekaran N. Antimicrobial activity of aluminium oxide nanoparticles for potential clinical applications. In: Mendez-Vilas A, editor. Science against microbial pathogens: communicating current research and technological advances, vol. 1. FORMATEX Microbiology Series No. 3; 2011. p. 245–51.

Norris DJ, Efros A, Erwin SC. Doped nanocrystals. Science 2008;319:1776–9.

Patten CL, Glick BR. Role of *Pseudomonas putida* indoleacetic acid in development of the host plant root system. Appl Environ Microbiol 2002;68:3795–801.

Rossbach S, Wilson TL, Kukuk ML, Carty HA. Elevated zinc induces siderophore biosynthesis genes and a *zntA*-like gene in *Pseudomonas fluorescens*. FEMS Microbiol Lett 2002;191:61–70.

Spencer M, Ryu CM, Yang K-Y, Kim YC, KloepperJ, Anderson AJ. Induced defence in tobacco by *Pseudomonas chlororaphis* strain O6 involves at least the ethylene pathway. Mol Plant Microbe Interact 2003;63:27–34.

Suchea S, Christoulakis M, Katsarakis N, Kitsopoulos T, Kiriakidis G. Comparative study of zinc oxide and aluminum doped zinc oxide transparent thin films grown by direct current magnetron sputtering. Thin Solid Films 2007;515:6562–6.

van Loon LC, Bakker PA, van der Heijdt WH, Wendehenne D, Pugin A. Early responses of tobacco suspension cells to rhizobacterial elicitors of induced systemic resistance. Mol Plant Microbe Interact 2008;21:1609–21.

Vansuyt G, Robin A, Briat J-F, Curie C, Lemanceau P. Iron acquisition from Fe-pyoverdine by *Arabidopsis thaliana*. Mol Plant Microbe Interact 2007;20:441–7.

Wahab R, Mishra A, Yun SI, Kim YS, Shin HS. Antibacterial activity of ZnO nanoparticles prepared via non-hydrolytic solution route. Appl Microbiol Biotechnol 2010;87:1917–25.

Wang H, Wick RL, Xing B. Toxicity of nanoparticulate and bulk ZnO, Al_2O_3 and TiO_2 to the nematode *Caenorhabditis elegans*. Environ Pollut 2009;157:1171–7.